Pergamon

Ocean Engineering 26 (1999) 125–145

OCEAN ENGINEERING

Full scale decay test of a tanker: field data and theoretical analysis

K. Nishimoto[a,*], F. Kaster[b], I.Q. Masetti[b], J. Matsuura[a], J.A.P. Aranha[a]

[a]*Department of Naval Architecture and Ocean Engineering, EPUSP, Sao Paulo, S.P., Brazil*
[b]*PETROBRÁS, Rio de Janeiro, R.J., Brazil*

Received 4 April 1997; accepted 20 August 1997

Abstract

This paper presents results from a full scale decay test made with a tanker in a relatively protected area in the Brazilian coast. In at least two tests the environmental loads (wind, waves and current) were very small and the time history of the surge motion was well behaved, making it possible to check some proposed models for the damping in the hull and mooring lines. Field data seem to confirm that the damping is indeed of the fluid viscosity type and the theoretical models are able to recover roughly 75% of the observed damping, the energy dissipation in the mooring lines being, by far, the major contribution. The remaining 25% are likely due to non modeled effects, such as the environment influence, which although small and not measured certainly exists, and to the friction between the mooring lines and the seabed.
© 1998 Published by Elsevier Science Ltd. All rights reserved.

Keywords: Full scale decay test; Floating production unit; Mooring line damping; Hull damping; Tanker

1. Introduction

The design of the mooring line system of a floating production unit depends strongly on the amplitude of the slow drift motion, that being a resonant phenomenon is very much affected by the damping of the unit. As it is known, the damping is

* Corresponding author.

0029-8018/99/$—see front matter © 1998 Published by Elsevier Science Ltd. All rights reserved.
PII: S0029-8018(97)10006-3

in general small and it is influenced by several distinct mechanisms, some of them difficult to be precisely estimated in a theoretical approach.

Roughly speaking, one can identify a first source of damping in the fluid viscosity, related to the drag forces that the submerged portions of the unit (hull, mooring lines and risers) experience when moving through the water and the emerged one when moving through the air. A second source of damping can be identified with the friction between the seabed and the mooring lines and a third one is of potential origin, related to the change of the drift forces caused by the slow motion of the unit.

This last component, named wave drift damping in the specialized literature, has deserved considerable attention lately, not only because it has an appreciable magnitude when compared with the others but also due to the fact that it is the only parcel that can be strictly computed with available software. The pertinent theory can be found in Grue and Palm (1993) and, as shown by Aranha (1994, 1996), the coefficients of the wave drift damping matrix can be exactly determined from the standard drift force coefficients in harmonic waves.

Among the remaining components, one that has deserved particular attention is the damping in the mooring lines, specially the influence of the first order (wave frequency) motion on the effective drag coefficient for the low frequency motion (see, for example, Huse and Matsumoto, 1989; Nakamura et al., 1991; Triantafyllou et al., 1994). The friction between seabed and the mooring line has been less studied but some approximations have been proposed (see, for example, Thomas and Hearn, 1994).

Most of the theoretical models have been contrasted with experimental results obtained in a laboratory condition. Wave drift damping, in particular, has been first observed experimentally by Wichers (1982) and the proposed models for mooring line damping have been compared, as a rule, against experimental results, as quoted in the above mentioned references. Besides these experimental studies under controlled conditions, it is certainly desirable to know how the models compare with the behavior of the real system. In spite of this, few data about the actual damping coefficient at full scale are known, mostly because the simultaneous effects of distinct environmental loads make it difficult to properly interpret the measurements.

In October 1995, PETROBRÁS conducted a four-day program to measure the damping of a tanker moored in a relatively protected area in the Brazilian coast. The motivation was to certify that the damping coefficients used in the mathematical models were properly estimated, as once it was thought they were generally too small. The idea was to carry out the standard decay test by pulling the moored tanker in the surge direction and then releasing it, in order to measure the decay rate in the time history of the surge motion. In the majority of these tests, the simultaneous action of the wave, ocean current and wind blurred the signal, making it difficult to properly evaluate the decay rate. By chance, however, some of the tests were made under conditions where the environmental loads were very weak, in such a way that a relatively clear signal of the surge motion could be observed and the damping coefficient could be obtained with some certainty.

The purpose of this paper is to present these results, together with relatively simple mathematical models and, by comparing them, to infer the ability the models have

to predict the actual damping. In Section 2, the theoretical background is elaborated, dealing both with the decay law of a single degree of freedom system with nonlinear damping and with damping models for the energy dissipation in the mooring lines, hull and for the observed small coupling between surge and sway motion. Section 3 presents particular features of the analyzed system, together with field data obtained and comparison with the theoretical model. Some final conclusions are presented in Section 4.

2. Mathematical models

This section presents the different mathematical models used in the analysis of field data. In Section 2.1, the decay law of a single degree of freedom system with a nonlinear damping is analyzed with the aim of identifying the preponderant damping mechanism observed in the full scale tests. In Sections 2.2–2.4, the damping models for the mooring lines, hull and the small coupling between surge and sway motion are elaborated and a brief summary is presented in Section 2.5.

2.1. The decay law for a nonlinear damping

One considers here the solution of the equation

$$m\ddot{x} + F(\dot{x}) + Rx = 0;\ \omega_n = \sqrt{\frac{R}{m}}; \tag{1a}$$

$$x(0) = A_0;\ \dot{x}(0) = 0,$$

where the damping function $F[\dot{x}]$ satisfies the dissipation condition:

$$F(\dot{x}).\dot{x} \geq 0. \tag{1b}$$

Assuming a small damping and a harmonic oscillation $x(t) = A\cos(\omega_n t)$ one can introduce the coefficient

$$\zeta(A) = \frac{\frac{1}{T_n}\int_0^{T_n} F(\dot{x}).\dot{x}\mathrm{d}t}{m\omega_n(\omega_n A)^2} << 1;\ T_n = \frac{2\pi}{\omega_n}, \tag{2a}$$

and consider, instead of Eq. (1a), the 'linear' equation

$$\ddot{x} + 2\zeta(A)\omega_n\dot{x} + \omega_n^2 x = 0, \tag{2b}$$

$$x(0) = A_0;\ \dot{x}(0) = 0.$$

Obviously, the energy dissipated by Eq. (1a) and Eq. (2b) are the same in one cycle and, if the damping is small, one can assume the solution of Eq. (2b) as being harmonic with an amplitude slowly varying with time, or $x(t) = A(T)\cos(\omega_n t)$ with

$T = \epsilon t$, where $\epsilon \cong O(\zeta(A)) \ll 1$. Placing this expression into Eq. (2b), and disregarding terms of order ϵ^2, one obtains the following decay law for the nonlinear damping:

$$\int_{A_0}^{A(t)} \frac{dA}{A.\zeta(A)} = -\omega_n t. \tag{2c}$$

Consider first a damping due to the fluid viscosity, that can be modeled as

$$F(\dot{x}) = c|\dot{x}|\dot{x}, \tag{3a}$$

leading to an equivalent local linear damping given by (see Eq. (2a))

$$\zeta_{FV}(A) = \frac{4}{3\pi}\frac{cA}{m}. \tag{3b}$$

In this case the equivalent damping coefficient diminishes, as it should, with the oscillation amplitude. Placing Eq. (3b) into Eq. (2c) and defining

$$\zeta_{FV} = \zeta_{FV}(A_0) = \frac{4}{3\pi}\frac{cA_0}{m}, \tag{3c}$$

the decay law for the oscillation amplitude can be given in the form

$$\frac{A_n}{A_0} = \frac{1}{1 + (2\pi\zeta_{FV})n}, \tag{3d}$$

where A_n is the amplitude of the nth crest.

The dry friction damping with the seabed can be modeled as

$$F(\dot{x}) = N.(\text{signal } \dot{x}), \tag{4a}$$

leading to the result

$$\zeta_{DF}(A) = \frac{2}{\pi}\frac{N}{m\omega_n^2 A}. \tag{4b}$$

In this case the equivalent linear damping has an opposite behavior to the one observed before, since it increases as the amplitude decreases. If one defines again

$$\zeta_{DF} = \zeta_{DF}(A_0) = \frac{2}{\pi}\frac{N}{m\omega_n^2 A_0} \tag{4c}$$

the following decay law can be derived in the case:

$$\frac{A_n}{A_0} = 1 - (2\pi\zeta_{DF})n. \tag{4d}$$

The results presented here can be confirmed by a direct simulation of Eq. (1a) and they are useful not only to help identify the main mechanism of damping in the full scale test, but also to check the predictive ability of the mathematical models.

2.2. Dissipation in the mooring lines

Suppose that h is the water depth, ℓ is the suspended length of the mooring line and $\theta_a = \arcsin(h/\ell)$. Let T_a be the traction in the mooring line at the point where the angle $\theta(s)$ with the horizontal is equal to θ_a; assuming that the suspended length between this point and the seabed is $\ell/2$ and ignoring the difference between the weight in air and water, by equilibrium one has $T_a(h/\ell) \cong mg(\ell/2)$, where m is the mass per unit of length. On the other hand, if the added mass is also disregarded, the wave velocity in the line is given by $c \cong (T_a/m)^{1/2} \cong (2\ell/T_{n,c})$, where $T_{n,c}$ is the natural period of the line. From these relations one obtains

$$T_{n,c} \approx 3\sqrt{\frac{h}{g}},$$

and so $T_{n,x}/T_{n,c} \ll 1$ even in deep water, where $T_{n,x} \approx 150\ s$ is the natural period of the surge motion. It turns out then that in the slow drift motion of the unit the mooring line motion can be modeled as a quasi-steady displacement, an approach that will be taken in the following.

2.2.1. In-plane displacement

The purpose here is to estimate the dissipation in the line due to an in-plane motion caused by the slow drift motion of the unit. In doing so one must consider, as explained above, the quasi-steady displacement along the catenary due to an imposed displacement at the suspended end. In particular, since the interest is focused on the drag force, one should be concerned with the displacement in the direction normal to the line. Considering the geometric and dynamic definitions indicated in Fig. 1, the equilibrium configuration is described by the equations of the catenary

$$tg\ \theta(s) = \frac{qs}{F_x},$$

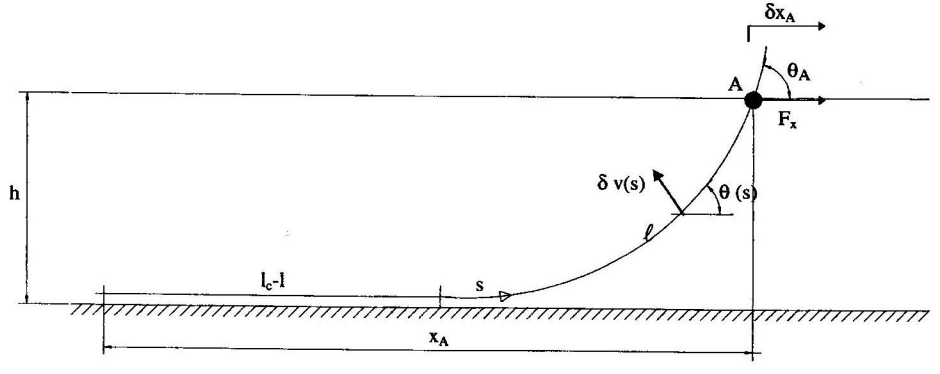

Fig. 1. Geometric and dynamic definitions of a catenary (q = submerged weight).

$$x(s) = (l_c - l) + \frac{F_x}{q}\sinh^{-1}\left(\frac{qs}{F_x}\right), \tag{5a}$$

$$y(s) = \frac{F_x}{q}\left[\sqrt{1 + \left(\frac{qs}{F_x}\right)^2} - 1\right];$$

in particular, the displacements at the suspended length A are given by

$$x_A = (l_c - l) + \frac{F_x}{q}\sinh^{-1}\left(\frac{ql}{F_x}\right), \tag{5b}$$

$$y_A = \frac{F_x}{q}\left[\sqrt{1 + \left(\frac{ql}{F_x}\right)^2} - 1 = h.\right]$$

Taking now the variation of Eq. (5b) with respect to F_x and ℓ, observing that $\delta y_A = 0$ and letting $R_H = \delta F_x/\delta x_A$ be the horizontal stiffness, one obtains

$$\frac{R_H}{q} = \frac{1}{\sinh^{-1}(\tan\theta_A) - 2\dfrac{1-\cos\theta_A}{\sin\theta_A}};$$

$$\delta l = \frac{1-\cos\theta_A}{\sin\theta_A}\frac{R_H}{q}\delta x_A. \tag{6a}$$

Repeating the same procedure with $(x(s);y(s))$, the following results can be derived:

$$\delta x(s) = \left[\sinh^{-1}(\tan(\theta(s)) - (1-\cos\theta(s))\frac{1-\cos\theta_A}{\sin\theta_A} - \sin\theta(s)\right]\frac{R_H}{q}\delta x_A;$$

$$\delta y(s) = \left[\frac{1-\cos\theta(s)}{\cos\theta(s)} + \sin\theta(s)\frac{1-\cos\theta_A}{\sin\theta_A} - \frac{\sin^2\theta(s)}{\cos\theta(s)}\right]\frac{R_H}{q}\delta x_A. \tag{6b}$$

Notice that $(\delta x(\ell) = \delta x_A;\ \delta y(\ell) = 0)$ and $(\delta x(0) = \delta y(0) = 0)$, since the variation of the touchdown point position is of second order in δx_A. The displacement in the normal direction $\delta v(s)$ is given by $\delta v(s) = -\sin\theta(s).\delta x(s) + \cos\theta(s).\delta y(s)$ and so

$$\delta v(s) = f(\theta(s))\frac{R_H}{q}\delta x_A;$$

$$f(\theta) = \frac{1-\cos\theta_A}{\sin\theta_A}\sin\theta - \sin\theta.\sinh^{-1}(\tan\theta) + (1-\cos\theta). \tag{6c}$$

If F_a is the horizontal drag force that the line applies to the system, C_D is the drag coefficient and D the line diameter, the dissipated power can be written as

$$\boldsymbol{P} = \int_0^1 \frac{1}{2}\rho C_D D|\delta\dot{v}(s)|(\delta\dot{v}(s))^2 \mathrm{d}s = F_a.\delta\dot{x}_A$$

and so

$$F_a = \frac{1}{2}\rho C_D D h.\gamma.|\delta\dot{x}_A|\delta\dot{x}_A, \tag{7a}$$

$$\gamma = \left(\frac{R_H}{q}\right)^3 \frac{1}{h}\int_0^1 |f(\theta(s))|.f^2(\theta(s))\mathrm{d}s.$$

Observing that $\mathrm{d}\theta = \cos^2\theta(q/F_x)\mathrm{d}s$, the result below can be derived:

$$\gamma = \left(\frac{R_H}{q}\right)^3 \frac{\cos\theta_A}{1-\cos\theta_A}\int_0^{\theta_A} \frac{|f(\theta)|.f^2(\theta)}{\cos^2\theta}\,\mathrm{d}\theta \cong \frac{\theta_A^5}{560}\left(\frac{R_H}{q}\right)^3. \tag{7b}$$

Fig. 2 presents the plot of γ as a function of θ_A together with the approximated expression given at the right side of Eq. (7b).

2.2.2. Out of plane displacement

Let δy_A be the displacement imposed in the plane perpendicular to the plane of the line. If the friction between the line and the seabed is ignored, one must consider that the line slips on the ground, pivoted at the anchor placed at $s = -\ell_c$. Ignoring

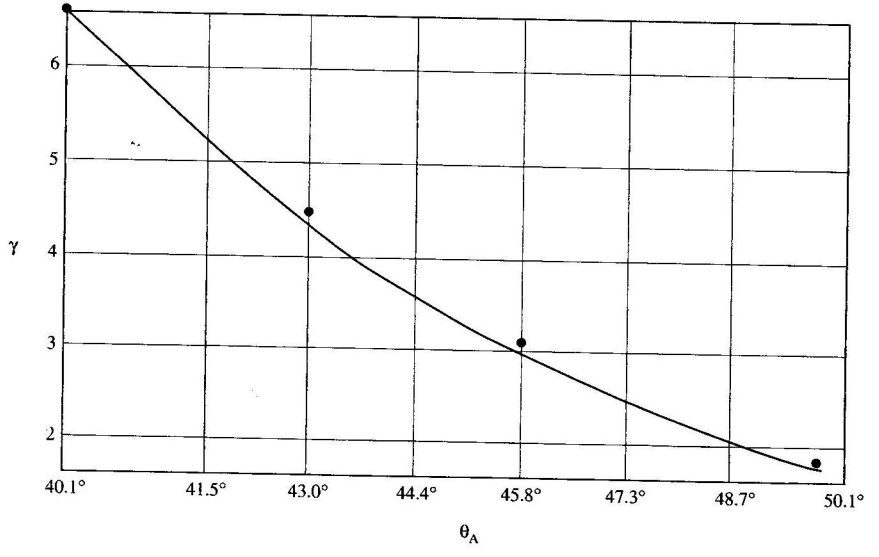

Fig. 2. The function $\gamma(\theta_A)$ and the approximation given in (7b).

also the fluid drag on the segment of the line that rests on the ground, but assuming that ℓ is relatively smaller than $\ell + \ell_c$, the displacement at each point of the line is roughly equal to δy_A, leading to the following expression for the drag force applied at A:

$$F_a = \frac{1}{2}\rho C_D Dl|\delta\dot{y}_A|\delta\dot{y}_A = \frac{1}{2}\rho C_D Dh\frac{\sin\theta_A}{1-\cos\theta_A}|\delta\dot{y}_a|\delta\dot{y}_A. \tag{8}$$

2.2.3. Global damping

One considers now a mooring line system with N lines, each line being characterized by the parameters $\{R_{H,i};\ \theta_{A,i};\ \gamma_i;\ \beta_i;\ i = 1,2,...,N\}$, with β_i being the angle that the plane of the line makes with the x-axis of the floating production system. If $\dot{x}$ is the surge velocity, it follows that

$$\boldsymbol{P} = F_x\dot{x} = \frac{1}{2}\rho C_D Dh\sum_{i=1}^{N}\left[\gamma_i|\delta\dot{x}_{A,i}|(\delta\dot{x}_{A,i})^2 + \frac{\sin\theta_{A,i}}{1-\cos\theta_{A,i}}|\delta\dot{y}_{A,i}|(\delta\dot{y}_{A,i})^2\right]$$

Observing the geometric relations

$$\delta\dot{x}_{A,i} = \dot{x}\cos\beta_i;$$

$$\delta\dot{y}_{A,i} = \dot{x}\sin\beta_i$$

and introducing the coefficient

$$\Gamma = \frac{1}{N}\sum_{i=1}^{N}\left[\gamma_i|\cos\beta_i|\cos^2\beta_i + \frac{\sin\theta_{A,i}}{1-\cos\theta_{A,i}}|\sin\beta_i|\sin^2\beta_i\right] \tag{9a}$$

the global surge force due to the energy dissipated in the mooring lines can be expressed as

$$F_x - \frac{\Gamma}{2}\rho C_D(ND)h|\dot{x}|\dot{x}. \tag{9b}$$

Recalling that the mass of the unit is given by $M = \rho C_B LBT$, L being the ship length, B the beam and T the draft, and if $C_{M,x}$ is the added mass coefficient in surge, then from Eq. (3c) one has

$$\zeta_{x,ML} = \frac{1}{1+C_{M,x}}\frac{2\Gamma}{3\pi}\frac{C_D}{C_B}\frac{h}{L}\frac{ND}{T}\frac{A_0}{B}, \tag{9c}$$

A_0 being the initial amplitude of the imposed motion, see Eq. (1a).

2.2.4. Damping in sway

The field data show that the observed free oscillations were not exclusively in surge, since a small sway motion could also be measured. This coupling is likely to be due to some unavoidable, although small, lack of symmetry in the mooring system and it should be accounted for in the analysis. With this purpose in mind, the damping in sway due to the mooring line is briefly discussed in the following.

Observing that the sway velocity, being much smaller than the surge velocity, should not affect in first order the intensity of the drag force, but only its direction, one can write

$$F_y = F_x \frac{\dot{y}}{\dot{x}} = \frac{\Gamma}{2} \rho C_D(ND) h |\dot{x}| \dot{y},$$

leading to the following expression for the nondimensional damping factor:

$$\zeta_{y,ML} = \frac{1 + C_{M,x}}{1 + C_{M,y}} \frac{\omega_x}{\omega_y} \zeta_{x,ML}. \tag{10}$$

In the above relation $C_{M,y}$ is the added mass coefficient in sway and ω_y the corresponding natural period assuming uncoupled modes.

2.3. Dissipation in the hull

In the surge motion, the velocity is given by $u(t) = \omega_x A_0 . \sin(\omega_x t)$ with averaged value equal to $2/\pi(\omega_x A_0)$; the Reynolds number is then given by the expression

$$R_e = \frac{2}{\pi} \frac{\omega_x A_0 L}{\nu}. \tag{11a}$$

Typically $R_e \approx 4 \times 10^7$ in the cases analyzed and in this range of Reynolds number one may use Prandtl's formula for the friction coefficient. If some form drag effect is also incorporated and the area LT is used instead of the wetted surface S, the fluid resistance can be written as

$$C_f(R_e) \cong \frac{0.1}{R_e^{0.2}} \frac{S}{TL}; \tag{11b}$$

$$F_x = \frac{1}{2} \rho C_f(R_e) LT |\dot{x}| \dot{x},$$

leading to the following coefficient for the nondimensional damping:

$$\zeta_{x,H} = \frac{2}{3\pi} \frac{1}{1 + C_{M,x}} \frac{C_f(R_e)}{C_B} \frac{A_0}{B}. \tag{11c}$$

If C_Y is the lateral force coefficient, of order 1, the sway damping coefficient can be written as (see Eq. (10))

$$\zeta_{y,H} = \frac{1 + C_{M,x}}{1 + C_{M,y}} \frac{\omega_x}{\omega_y} \frac{C_Y}{C_f(R_e)} \zeta_{x,H}. \tag{12}$$

Notice that here $\zeta_{y,H} \gg \zeta_{x,H}$ since $C_Y \gg C_f(R_e)$.

2.4. Modal coupling

The mooring system is, in general, arranged in a symmetrical pattern around the longitudinal axis and, as a consequence, the surge and sway modes of motion are

theoretically uncoupled. In reality, however, some small asymmetry in the mooring system seems to be unavoidable, leading to a small coupling between these two modes of motions. This fact has been observed in the field measurements, where a small sway motion was detected together with the preponderant surge motion (field data show also that the coupling with the yaw motion can be ignored). Due to the discrepancy between $\zeta_{y,H}$ and $\zeta_{x,H}$ this coupling, although small, can be important in the computation of the global damping coefficient of the 'surge' motion. The purpose of this item is to estimate the influence of such coupling in the value of ζ.

First of all, one observes that the damping, although nonlinear, can be linearized for a time small enough; from Eq. (3d), for example, one obtains

$$\frac{A(t)}{A_0} = \frac{1}{1 + \zeta_{FV}(\omega_n t)} \cong 1 - \zeta_{FV}(\omega_n t) \cong e^{-\zeta_{FV}(\omega_n t)}$$

for $\zeta_{FV}(\omega_n t) \ll 1$. This observation justifies, at least in first approximation, to take a linear damping model in the analysis that follows.

Let $M_x = (1 + C_{M,x})M$ and $M_y = (1 + C_{M,y})M$ be the mass in surge and sway respectively and $(R_x;R_y)$ be the local restoring force coefficients in these directions. The natural frequencies are defined by the expressions

$$\omega_x = \sqrt{\frac{R_x}{M_x}};\ \omega_y = \sqrt{\frac{R_y}{M_y}},$$

and the free oscillation equation can be written in the form

$$\begin{bmatrix} M_x & 0 \\ 0 & M_y \end{bmatrix} \begin{Bmatrix} \ddot{x} \\ \ddot{y} \end{Bmatrix} + \begin{bmatrix} 2M_x\omega_x\zeta_x & 0 \\ 0 & 2M_y\omega_y\zeta_y \end{bmatrix} \begin{Bmatrix} \dot{x} \\ \dot{y} \end{Bmatrix} + \begin{bmatrix} R_x & R_{xy} \\ R_{xy} & R_y \end{bmatrix} \begin{Bmatrix} x \\ y \end{Bmatrix} = \begin{Bmatrix} 0 \\ 0 \end{Bmatrix}, \tag{13a}$$

with the coupling R_{xy} being small in the sense that

$$\delta = \frac{R_{xy}^2}{R_x \cdot R_y} \ll 1. \tag{13b}$$

The 'surge' natural frequency $\omega_{x,c}$ of the undamped system (13a) is given by

$$\left(\frac{\omega_{x,c}}{\omega_x}\right)^2 = 1 + \frac{\omega_y^2}{(\omega_x^2 - \omega_y^2)}\,\delta, \tag{14a}$$

while the natural mode is defined by the vector

$$\begin{Bmatrix} 1 \\ \alpha \end{Bmatrix};\ \alpha = \frac{R_{xy}}{R_y}\frac{\omega_y^2}{(\omega_x^2 - \omega_y^2)} \ll 1. \tag{14b}$$

The characteristic equation of Eq. (13a) has roots of the form $p = i\omega_{x,c}(1 + i\zeta)$ where ζ is the 'surge' damping in the coupled model. Ignoring terms of order $\zeta^2, \delta\zeta$, the following relation can be derived for ζ:

$$\zeta = \zeta_x + \frac{M_y}{M_x}\frac{\omega_y}{\omega_x}\alpha^2\zeta_y;$$

$$\alpha = \frac{\text{sway amplitude}}{\text{surge amplitude}}. \tag{14c}$$

The value of α can be estimated directly from the field data, by comparing the amplitudes of the sway and surge motions in the free oscillation experiment; from the estimated value of α the final damping coefficient ζ can be determined once the values of ζ_x and ζ_y are given.

2.5. Summary

As stated in the Introduction, the present work is concerned with the analysis of field data obtained from a decay test of a tanker under such conditions that the environmental loads were very weak. In these circumstances, the influence of these actions on the damping (wave drift damping, damping due to wind and ocean current) were ignored in the mathematical model, together with the seabed friction. In this way, only the damping in the mooring lines and in the ship hull were accounted for, leading to the expressions

$$\zeta_x = \zeta_{x,ML} + \zeta_{x,H} = \frac{1}{1 + C_{M,x}} \left[\frac{2\Gamma}{3\pi} \frac{C_D}{C_B} \frac{h}{L} \frac{ND}{T} + \frac{2}{3\pi} \frac{C_f(R_e)}{C_B} \right] \frac{A_0}{B},$$

$$\zeta_y = \zeta_{y,ML} + \zeta_{y,H} = \frac{1 + C_{M,x}}{1 + C_{M,y}} \frac{\omega_x}{\omega_y} \left[\zeta_{x,ML} + \frac{C_Y}{C_f(R_e)} \zeta_{x,H} \right]. \tag{15}$$

In Eq. (15) ($C_{M,x}$; $C_{M,y}$) are the added mass coefficients in surge and sway, (ω_x; ω_y) are the respective natural frequencies, C_BLBT is the displacement volume of the ship, C_Y its transversal drag coefficient, while $C_f(R_e)$ is the longitudinal one, see Eq. (11b); also, h is the water depth, N is the number of lines in the mooring system, D the line diameter and C_D its drag coefficient. The parameter Γ is defined in Eq. (7b) and (9b).

With these definitions the final damping coefficient can be determined by means of Eq. (14c).

3. Full scale experiment

The field program was conducted from 26/10/95 to 29/10/95 on a 30 kDWT tanker named *ALAGOAS*, moored with a relatively complacent system in a region on the south part of the Brazilian coast. Specifically, in the measurements made in 27/10/95, where the environmental loads were weaker, the ship was placed at 26° 46.75′S, 46° 48.35′W, heading 214° in relation to the true North. The ship position was registered by a DGPS-TRIMBLE system and the angular direction by a Rate Gyro; additionally, the ship was provided with accelerometers and inclinometers. The environmental condition was measured by a wave probe, by a current meter installed in a nearby ocean platform and by an anemometer placed at the ship; on 27/10/95

Table 1
ALAGOAS parameters

L	B	T	∇	S	C_B	$C_{M.x}$	$C_{M.Y}$	C_Y
168 m	25 m	7.6 m	27,428 m^3	4996 m^2	0.84	0.06	1.14	1.30

the wind speed was 7 knots, the wave height was smaller than 0.5 m and the ocean current smaller than 0.2 m/s.

The main dimensions of *ALAGOAS* are given in Table 1, together with pertinent hydrodynamic coefficients. Notice that the added mass coefficients have been computed numerically, while the transversal force coefficient C_Y has been taken, in this exercise, as being the averaged value of a rectangle's drag coefficient with $B/2T = 1.7$ (see Hoerner, 1975).

The mooring line system is characterized by the parameters shown in Table 2; notice that the immersed weight q, the diameter D and the drag coefficient C_D are averaged values, since the lines are made by a composition of chains and cables.

Each mooring line is defined also by the angle β of its plane with the longitudinal axis of the ship; in the case analyzed the values of β are $\{\beta = 40°; 75°; 135°; 140°; 220°; 225°; 285°; 320°;\}$.

The water depth was $h = 185$ m, the water density is $\rho = 1025$ kg/m^3 and $g = 9.81$ m/s^2.

3.1. Results from the decay test

Two decay tests will be analyzed. In the first, the ship was pulled from its original equilibrium position by a traction of 70 tonf and then released; in the second, the pulling force was 100 tonf. The instantaneous ship's position, determined from the DGPS system with a sampling rate of 3 s, was given in terms of the geographical coordinates and later transformed into surge and sway motions. The origin of the coordinated system was chosen in an arbitrary point along the path in the pulling operation and the instantaneous x,y-directions (surge and sway, respectively) was monitored by a Rate Gyro; the coordinates $(x(t),y(t))$ were then determined by projecting the position vector in these directions. Considerable difficulty in interpreting the measurements would arise if the change in heading were strong; the observed yaw motion, however, was very small and the instantaneous heading coincided, in essence, with the heading at equilibrium. Notice also that since the origin of the

Table 2
Mooring line parameters

q	N	D	C_D
58 kgf/m	8	0.095 m	1.80

coordinated system was placed at an 'arbitrary' point, the coordinates $(x(t),y(t))$ were not related to the equilibrium position; in fact, the coordinates of the equilibrium point must be inferred from the field data, as shown in Section 3.2.

Fig. 3(a) presents the ship's path in the (x,y) plane when the pulling force was 70 tonf, while Fig. 3(b) presents the time history $y(t)$ of the sway motion; Fig. 4(a,b)

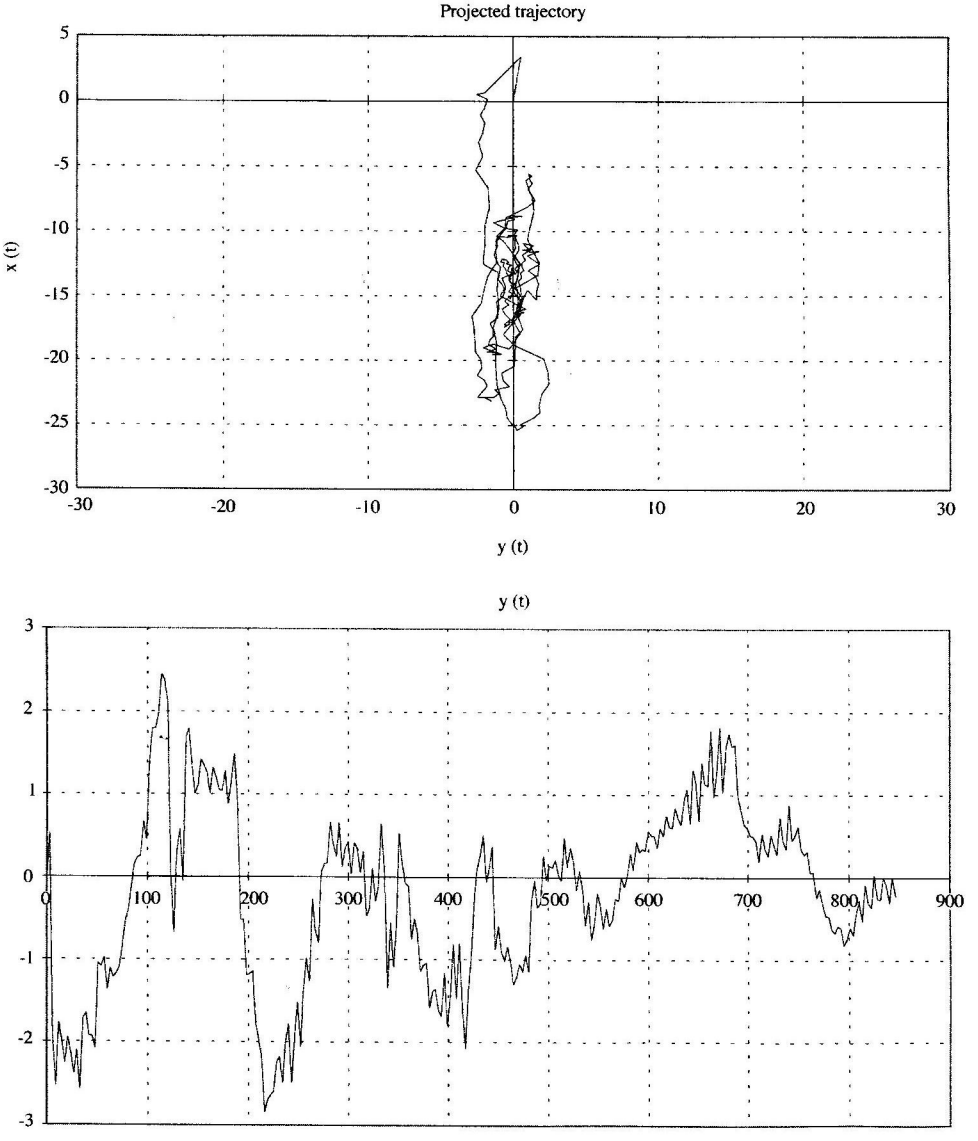

Fig. 3. (a) Ship's path in the (x,y) plane; (b) sway motion. —Case: 70 tonf.

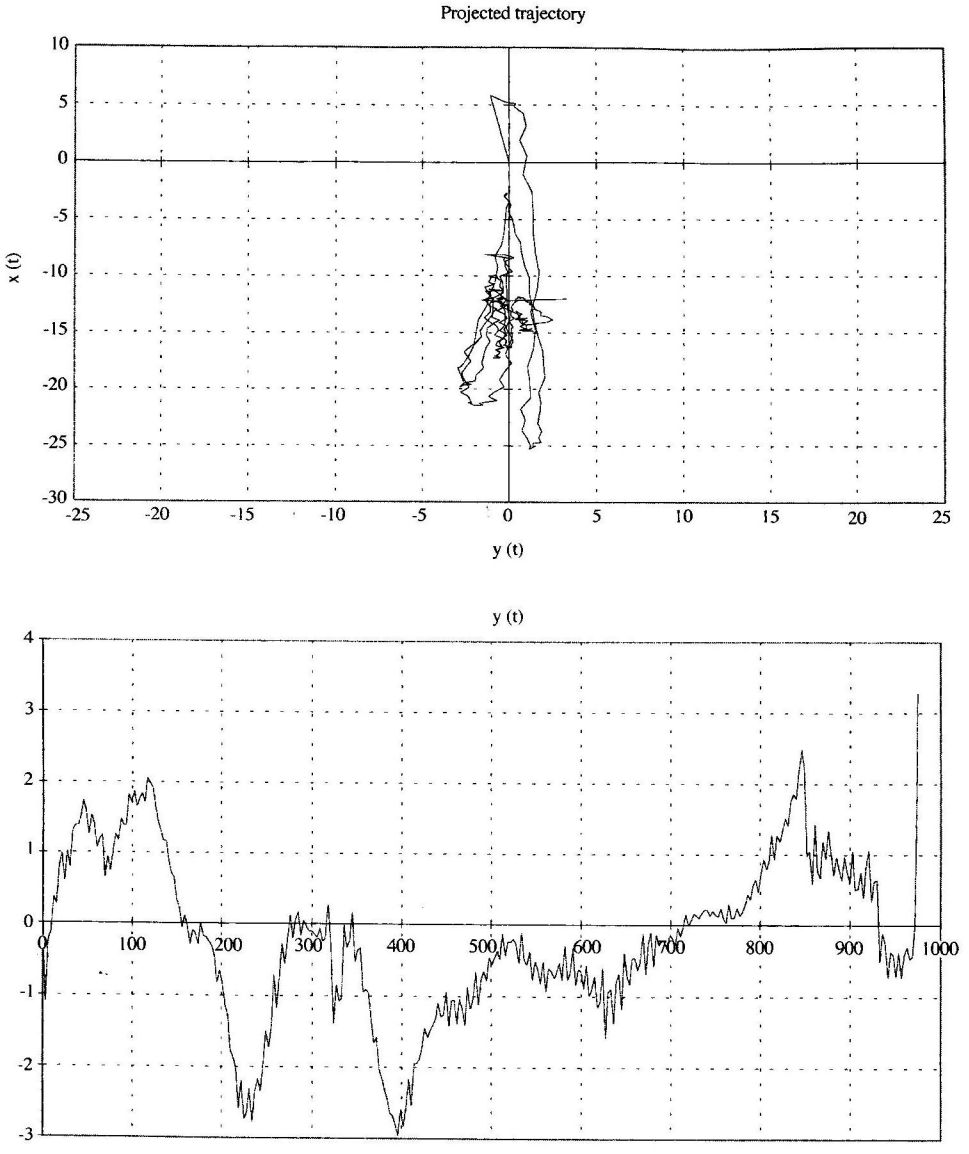

Fig. 4. (a) Ship's path in the (x,y) plane; (b) sway motion. —Case: 100 tonf.

repeat the same data for the case where the pulling force was 100 tonf. The surge motion $x(t)$ for both cases are presented in Fig. 5.

The coupled model discussed in Section 2.4 predicts a path in the (x,y) plane that should coincide with a slender ellipse, slightly skewed in relation to the axis and slowly spiralling around the equilibrium point. The field data is not fully disappointing in this respect, even more if one observes the inherent imprecision in the

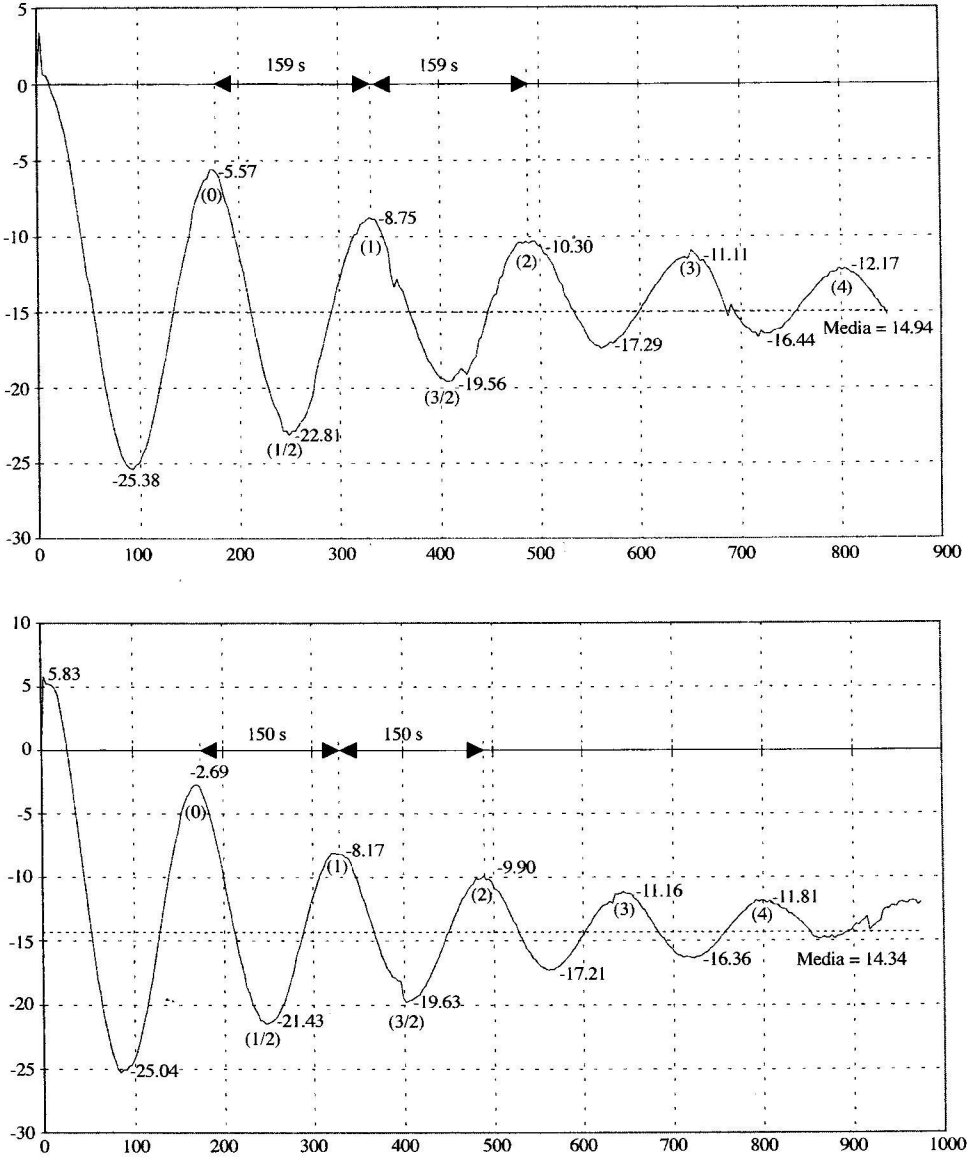

Fig. 5. (a) Surge motion —Case 70 tonf; (b) surge motion —Case 100 tonf.

determination of the y-coordinate, of the order of magnitude of the DGPS precision. The observed ratio between sway and surge motions is roughly of order 1:4 in both cases ($\alpha \approx 0.25$ in Eq. (14c)) and a detailed analysis of the surge motion $x(t)$ will be made next.

3.2. Analysis of the surge motion

Although the sway time history is a little erratic, the surge time history $x(t)$ is very well behaved, considering the source of the data, namely, the fact that one is dealing with full scale measurements made at sea. The first crest, near the time $t = 0$, was not considered in the analysis, since it is influenced by the 'releasing operation', where the traction is alleviated until it reaches the zero value. One considers then the oscillation as if started in the second crest, named the 0-crest in the following, and the subsequent crests $n = 1,2,3,4$; the troughs are numbered $n = 1/2,3/2,5/2,7/2$, indicating a time lag of $n.T_{n,x}$ from the 0-crest.

Assuming a small damping, the equilibrium point has a coordinate $\langle x \rangle$ that can be estimated by the expression

$$\langle x \rangle = \frac{1}{2}\left[\frac{x_{1/2} + x_{3/2}}{2} + x_1\right]$$

and from the field data one obtains

$$\langle x \rangle_{70} = -14.94 \text{ m}; \qquad \langle x \rangle_{100} = -14.34 \text{ m}. \tag{16a}$$

Two damping mechanisms have been considered here: one, of fluid viscosity origin, has the general form (3a) and obeys the decay law (3d) with ζ_{FV} defined by Eq. (3c); the other, of dry friction origin, is defined by Eq. (4a) and obeys the decay law (4d) with ζ_{DF} defined by Eq. (4c). From the observed ratio A_n/A_0 one can determine both damping coefficients by the formulas

$$\zeta_{FV} = \frac{1}{2\pi n}\left(\frac{A_0}{A_n} - 1\right); \qquad \zeta_{DF} = \frac{1}{2\pi n}\left(1 - \frac{A_n}{A_0}\right). \tag{16b}$$

The idea now is to use the empirical data, together with Eq. (16b), to obtain information about the preponderant damping mechanism in the full scale test. Specifically, one can check first if the empirical data can be fitted to any of these expressions; if this is the case, one can then infer which damping mechanism is the preponderant one.

One could obviously derive, from Eq. (2c, 3b and 4b), a general decay law, considering both the fluid viscosity and dry friction damping; this route, however, will not be pursued here, but will be briefly addressed at the end of this section.

3.2.1. Crest decay law

Let x_n be the coordinate of the nth crest; its amplitude will be $A_n = x_n - \langle x \rangle$, where the values of $\langle x \rangle$ are given in Eq. (16a). From Fig. 5 and Eq. (16a) one can compute then the values of the damping coefficients Eq. (16b) for each n, the final result being shown in Table 3.

Table 3
Results from the full scale decay test

n	A_n	A_n/A_0	ζ_{DF}	ζ_{FV}
70 tonf; crests				
0	9.37 m	1	*	*
1	6.19 m	0.661	0.054	0.082
2	4.64 m	0.495	0.040	0.081
3	3.83 m	0.409	0.031	0.077
4	2.77 m	0.296	0.028	0.095
				0.084
100 tonf; crests				
0	11.65 m	1	*	*
1	6.17 m	0.530	0.075	0.141
2	4.44 m	0.381	0.049	0.129
3	3.18 m	0.273	0.039	0.141
4	2.53 m	0.217	0.031	0.143
				0.138

Two facts should be noticed here: first, the actual damping cannot be fitted to the dry friction model, since ζ_{DF} changes strongly with n; on the other hand, the observed damping closely follows the algebraic decay law (3c), related to the fluid viscosity damping. In fact, in this case the normalized standard deviation (namely, the standard deviation divided by the averaged value) is of the order of 16% for the 70 tonf experiment and of order of 8% in the 100 tonf case.

As a conclusion, the field data seem to indicate that the actual damping mechanism is dominated by fluid viscosity, as defined in Eq. (3a).

3.2.2. *Decay behavior of the troughs*

An interesting, yet unexplained, aspect of the obtained field data is the somewhat erratic behavior of the trough decay law. As shown in Table 4, the damping mech-

Table 4
Results from the full scale decay test

n	A_n	A_n/A_0	ζ_{DF}	ζ_{FV}
70 tonf; troughs				
0	9.37 m	1	*	*
1/2	7.87 m	0.840	0.051	0.061
3/2	4.62 m	0.493	0.054	0.110
5/2	2.35 m	0.251	0.050	0.191
7/2	1.50 m	0.160	0.038	0.234
100 tonf; troughs				
0	11.65 m	1	*	*
1/2	7.09 m	0.609	0.124	0.204
3/2	5.29 m	0.454	0.058	0.128
5/2	2.87 m	0.246	0.048	0.195
7/2	2.02	0.173	0.038	0.217

anism is apparently dominated by the dry friction model in the 70 tonf case (normalized standard deviation equal to 25%) and by the fluid viscosity model in the 100 tonf case (normalized standard deviation equal to 37%). Although there may exist some physical reason for this distinct behavior, as for example the non symmetry of the mooring line system with respect to y-axis or even the dependence of the actual friction on the direction of the displacement, imprecision in the measurements should not be ruled out.

The fact is that one could not detect a clear pattern in the trough decay law and, for this reason, only the crest data will be taken as being representative of the physical phenomenon.

3.3. Comparison with mathematical model

In this section the expressions for the damping due to the mooring lines and hull will be applied to the case under consideration, to check if they can provide the correct order of magnitude. In spite of the apparent completeness of the theory, a working hypothesis about the mooring line system is needed. In fact, the actual pre-tension in each mooring line was not monitored and so one has just one equation (measured natural period) to determine the eight values of the local stiffens $\{R_{H,i};\ i = 1,..,8\}$. To overcome this difficulty one must assume, as a working hypothesis, that the pre-tension in the lines are the same. In this way one has

$$R_x = R_H \sum_{i=1}^{N} \cos^2\beta_i = 3.48 R_H;$$

$$R_y = R_H \sum_{i=1}^{N} \sin^2\beta_i = 4.52 R_H, \tag{17a}$$

and, by definition, the natural frequencies in surge and sway are related by the expression

$$\frac{\omega_x}{\omega_y} = \sqrt{\frac{1 + C_{M,x}}{1 + C_{M,y}} \frac{R_x}{R_y}} = 1.25. \tag{17b}$$

From the natural periods observed in the field data (see Fig. 5), one can infer the stiffness R_x and so the value of R_H; it turns out that

$$\left(\frac{R_H}{q}\right)_{70} = 23.5;\ (\theta_A)_{70} \cong 0.750\text{rad} \Rightarrow \gamma_{70} = 5.5;$$

$$\left(\frac{R_H}{q}\right)_{100} = 26.5;\ (\theta_A)_{100} \cong 0.725\text{rad} \Rightarrow \gamma_{100} = 6.7. \tag{18a}$$

From these results one obtains

$$\Gamma_{70} = 2.90 \Rightarrow (\zeta_{x,ML})_{70} = 0.14 \frac{A_0}{B};$$

$$\Gamma_{100} = 3.33 \Rightarrow (\zeta_{x,ML})_{100} = 0.16 \frac{A_0}{B}. \tag{18b}$$

Using now the hull expression for the damping, see Eq. (11c) with $R_e = 45\text{x}10^6$, one gets

$$\zeta_{x,H} = 0.003 \frac{A_0}{B} \tag{18c}$$

and so, from Eq. (15), it follows that

$$(\zeta_x)_{70} = 0.143 \frac{A_0}{B}\ ;\ (\zeta_x)_{100} = 0.163 \frac{A_0}{B}\ ; \tag{18d}$$

$$(\zeta_y)_{70} = 0.330 \frac{A_0}{B}\ ;\ (\zeta_y)_{100} = 0.342 \frac{A_0}{B}.$$

From these expressions and Eq. (14c), with $\alpha = 0.25$, one finally obtains

$$\zeta_{70} = 0.185 \frac{A_0}{B} \Rightarrow \zeta_{70} = 0.069;$$

$$\zeta_{100} = 0.206 \frac{A_0}{B} \Rightarrow \zeta_{100} = 0.096. \tag{19}$$

The predicted values correspond to 82% of the measured one in the 70 tonf case and to 70% in the 100 tonf test.

3.4. *Qualitative influence of the non modeled effects*

One hopes that the algebraic decay law (3d), related to the fluid viscosity mechanism and apparently followed by the field data, should remain essentially correct when small non modeled effects are considered in the theory; otherwise, the complete mathematical model, where these effects are incorporated, would be unable to cope with the empirical data and would be of little importance to describe the actual behavior of the physical system.

To check this point one considers here a damping of more general form, given by

$$\zeta(A) = \zeta_{FV} \frac{A}{A_0} + \zeta_{EN} + \zeta_{DF} \frac{A_0}{A}, \tag{20a}$$

where supposedly ζ_{EN} models the environment influence and ζ_{DF} the friction with the seabed; these parcels can be ignored in a first order (simplified) model only if

$$\epsilon_1 = \frac{\zeta_{EN}}{\zeta_{FV}} \ll 1;\ \epsilon_2 = \frac{\zeta_{DF}}{\zeta_{FV}} \ll 1. \tag{20b}$$

Placing Eq. (20a) and (20b) in Eq. (2c) and defining $a = A/A_0$ one obtains

$$\int_{\frac{A_n}{A_0}}^{1} \frac{da}{a^2 + \epsilon_1 a + \epsilon_2} = 2\pi\zeta_{FV} n.$$

The above integral can be determined exactly; assuming, for instance, that $\epsilon_2 > (\epsilon_1/2)^2$ one obtains, after disregarding terms of order ϵ^2 when compared to 1, that

$$\frac{A_n}{A_0} = \frac{1}{1 + (2\pi\zeta)n}, \tag{20c}$$

$$\zeta = \zeta_{FV} + \zeta_{EN} + \zeta_{DF}.$$

It turns out that the non-modeled effects do not change, if small, the algebraic decay law (3c); their only effect is to increase the damping coefficient ζ_{FV} by a factor $(1 + \epsilon_1 + \epsilon_2)$.

4. Conclusion

From the results obtained in the full scale test and the pertinent mathematical models, the following conclusions can be drawn at this point:

1. The dry friction damping mechanism is apparently less important than the fluid viscosity damping mechanism; its importance, however, tends to increase as the amplitude of the oscillation diminishes, see Eq. (3c) and Eq. (4c);
2. The viscous dissipation in the mooring lines is, by far, the major sink of energy for the surge free oscillation when the environment influence is weak; furthermore, the quasi-steady approach to analyze the mooring line drag predicts a damping coefficient with the correct order of magnitude;
3. The theoretical model accounts for roughly 75% of the observed damping; the remaining parcel can well be accommodated with some non modeled effects, such as the environment influence and the friction with the seabed.

As a rule, relatively simple mathematical models can be used to infer the amount of damping with a precision that seems good from an engineering point of view. On the other hand, a more precise mathematical model could be very complicated, both conceptually and numerically, with a potential gain that does not seem to be impressive.

Acknowledgements

This work has been supported by PETROBRÁS under a general research program between this company and the Department of Naval Architecture and Ocean Engineering of EPUSP; the authors also acknowledge some useful suggestions made by Dr A.C. Fernandes.

References

Aranha, J.A.P., 1994. A formula for 'wave damping' in the drift of a floating body. J. Fluid Mech. 275, 147–155.

Aranha, J.A.P., 1996. Second-order horizontal steady forces and moment on a floating body with a small forward speed. J. Fluid Mech. 313, 39–54.

Grue, J., Palm, E., 1993. The mean drift forces and yaw moment on marine structure in waves and current. J. Fluid Mech. 150, 121–142.

Hoerner, S.F., 1975. Fluid-Dynamic Drag: Practical Information on Aerodynamic Drag and Hydrodynamic resistance. Published by the author.

Huse, E., Matsumoto, K., 1989. Mooring line damping due to first and second order vessel motion. OTC 6137, 21th Annual OTC, Houston, Texas, 1–4 May 1989.

Nakamura, N., Koterayama, W., Kyozuca, Y., 1991. Slow drift damping due to drag forces acting on mooring lines. Ocean Engng 18 (4), 283–296.

Thomas, D.O., Hearn, G.E., 1994. Deepwater mooring line dynamics with emphasis on seabed inteference effects. OTC 7488, 26th Annual OTC. Houston, Texas, 2–5 May 1994.

Triantafyllou, M.S., Yue, D.K.P., Tein, D.Y.S., 1994. Damping of moored floating structures. OTC 7489, 26th Annual OTC. Houston, Texas, 2–5 May 1994.

Wichers, J.E.W., 1982. On the low frequency surge motions of vessels moored in high seas. 14th Annual OTC. Houston, Texas.